

SANDIA REPORT

SAND201X-XXXX

Unlimited Release

Printed Month and Year

Assessing the Validity of the Simplified Potential Energy Clock Model for Modeling Glass-Ceramics

Ryan D. Jamison, Anne M. Grillet, Mark E. Stavig, Kevin Strong, and Steve Dai

Prepared by
Sandia National Laboratories
Albuquerque, New Mexico 87185 and Livermore, California 94550

Sandia National Laboratories is a multimission laboratory managed and operated by National Technology and Engineering Solutions of Sandia, LLC, a wholly owned subsidiary of Honeywell International, Inc., for the U.S. Department of Energy's National Nuclear Security Administration under contract DE-NA0003525.



Sandia National Laboratories

Issued by Sandia National Laboratories, operated for the United States Department of Energy by National Technology and Engineering Solutions of Sandia, LLC.

NOTICE: This report was prepared as an account of work sponsored by an agency of the United States Government. Neither the United States Government, nor any agency thereof, nor any of their employees, nor any of their contractors, subcontractors, or their employees, make any warranty, express or implied, or assume any legal liability or responsibility for the accuracy, completeness, or usefulness of any information, apparatus, product, or process disclosed, or represent that its use would not infringe privately owned rights. Reference herein to any specific commercial product, process, or service by trade name, trademark, manufacturer, or otherwise, does not necessarily constitute or imply its endorsement, recommendation, or favoring by the United States Government, any agency thereof, or any of their contractors or subcontractors. The views and opinions expressed herein do not necessarily state or reflect those of the United States Government, any agency thereof, or any of their contractors.

Printed in the United States of America. This report has been reproduced directly from the best available copy.

Available to DOE and DOE contractors from

U.S. Department of Energy
Office of Scientific and Technical Information
P.O. Box 62
Oak Ridge, TN 37831

Telephone: (865) 576-8401
Facsimile: (865) 576-5728
E-Mail: reports@osti.gov
Online ordering: <http://www.osti.gov/scitech>

Available to the public from

U.S. Department of Commerce
National Technical Information Service
5301 Shawnee Rd
Alexandria, VA 22312

Telephone: (800) 553-6847
Facsimile: (703) 605-6900
E-Mail: orders@ntis.gov
Online order: <https://classic.ntis.gov/help/order-methods/>



Assessing the Validity of the Simplified Potential Energy Clock Model for Modeling Glass-Ceramics

Ryan D. Jamison
Org. 06621

Anne M. Grillet
Org. 01513

Mark E. Stavig
Org. 01853

Kevin Strong
Org. 01851

Steve Dai
Org. 01833

Sandia National Laboratories
P. O. Box 5800
Albuquerque, New Mexico 87185

Abstract

Glass-ceramic seals may be the future of hermetic connectors at Sandia National Laboratories. They have been shown capable of surviving higher temperatures and pressures than amorphous glass seals. More advanced finite-element material models are required to enable model-based design and provide evidence that the hermetic connectors can meet design requirements. Glass-ceramics are composite materials with both crystalline and amorphous phases. The latter gives rise to (non-linearly) viscoelastic behavior. Given their complex microstructures, glass-ceramics may be thermorheologically complex, a behavior outside the scope of currently implemented constitutive models at Sandia. However, it was desired to assess if the Simplified Potential Energy Clock (SPEC) model is capable of capturing the material response.

Available data for SL 16.8 glass-ceramic was used to calibrate the SPEC model. Model accuracy was assessed by comparing model predictions with shear moduli temperature dependence and high temperature 3-point bend creep data. It is shown

that the model can predict the temperature dependence of the shear moduli and 3-point bend creep data. Analysis of the results is presented. Suggestions for future experiments and model development are presented. Though further calibration is likely necessary, SPEC has been shown capable of modeling glass-ceramic behavior in the glass transition region but requires further analysis below the transition region.

ACKNOWLEDGMENTS

The authors would like to thank Arthur Brown for funding the modeling effort through the ASC P&EM program and Kevin Ewsuk for providing funding for data collection. Also, thank you to Brenton Elisberg, Kurtis Ford, and Kevin Long for their assistance in calibrating the model to data. Lastly, thank you to our peer reviewers!

TABLE OF CONTENTS

1.	Introduction	13
2.	Experimental Data	15
2.1.	Dynamic Torsion Tests	15
2.2.	Dynamic Flexural Tests	18
2.3.	Thermal Strain Tests	19
2.4.	High Temperature Flexural Creep Tests	20
3.	Model Calibration	23
3.1.	Shear Master Curve	23
3.2.	3-Point Bend Temperature Sweep	25
3.3.	Thermal Strain	26
3.4.	SPEC Model Calibration	27
4.	Model Validation	29
4.1.	Shear Temperature Sweep	29
4.2.	High Temperature Creep	31
4.3.	Validation Summary	34
5.	Future Work	35
5.1.	Experimental	35
5.2.	Modeling	36
6.	Conclusion	37
	References 39	
	Appendix A: Prony Times and Weights	41

FIGURES

Figure 1. Measured Shear Storage Modulus at Various Temperatures.....	16
Figure 2. Measured Shear Loss Modulus at Various Temperatures.....	16
Figure 3. Measured Shear Tan Delta at Various Temperatures.....	17
Figure 4. Measured Temperature Dependence of the Shear Storage and Loss Moduli.	17
Figure 5. Measured Temperature Dependence of the Shear Tan Delta.....	18
Figure 6. Measured Temperature Dependence of the Tensile Storage and Loss Moduli.....	19
Figure 7. Measured Temperature Dependence of the Tensile Tan Delta.	19
Figure 8. Measured Thermal Strain Data for Various Cooling Rates.	20
Figure 9. Measured 3-Point Bend Creep at 460 °C at Several Stress Levels	21
Figure 10. Measured 3-Point Bend Creep at 550 °C at Several Stress Levels	21
Figure 11. Measured Creep Compliance at 460 °C at Several Stress Levels.	22
Figure 12. Measured Creep Compliance at 550 °C at Several Stress Levels.	22
Figure 13. Shifted Shear Storage and Loss Master Curves for a Reference Temperature of 650 °C.	23
Figure 14. Shifted Master Curve of the Shear Tan Delta for a Reference Temperature of 650 °C.	24
Figure 15. Log(a) Shift Factors for a Reference Temperature of 650 °C and the Williams-Landel-Ferry Fit.....	24
Figure 16. Vertical Shift Factors Used when Constructing the Shear Master Curve.	25
Figure 17. Comparison Between Measured Storage and Loss Moduli and the SPEC Model Fit for the 3-Point Bend Temperature Sweep.....	26
Figure 18. Comparison Between Measured Tan Delta and the SPEC Model Fit for the 3-Point Bend Temperature Sweep.	26
Figure 19. Comparison of the Experimentally Measured Thermal Strain and the Model Predicted Thermal Strain.....	27
Figure 20. Comparison Between the Measured Shear Storage And Loss Moduli and the SPEC Model Predictions for the Shear Temperature Sweep.....	30
Figure 21. Comparison Between the Measured Tan Delta and the SPEC Model Predictions for the Shear Temperature Sweep.....	30
Figure 22. Schematic of the 3-Point Bend Model.	31
Figure 23. Comparisons Between Measured Creep Strain (symbols) and SPEC Model (solid lines) Predictions for 3-Point Bend Creep at 460 °C.	32

Figure 24. Comparisons Between Measured Creep Compliance (symbols) and the SPEC Model (solid lines) Predictions for 3-Point Bend Creep at 460 °C.....	32
Figure 25. Comparisons Between the Measured Creep Strain (symbols) and the SPEC Model (solid lines) Predictions for 3-Point Bend Creep at 550 °C.....	33
Figure 26. Comparisons Between the Measured Creep Compliance (symbols) and the SPEC Model (solid lines) Predictions for 3-Point Bend Creep at 550 °C.....	34

TABLES

Table 1. SPEC Model Parameters for SL 16.8 Glass-Ceramic.	28
--	----

NOMENCLATURE

Abbreviation	Definition
BPS	Belt-Processed S-glass
CTE	Coefficient of thermal expansion
DMA	Dynamic Mechanical Analyzer
E_s	Tensile storage modulus
E_l	Tensile loss modulus
GcTMS	Glass-ceramic to metal seal
G_s	Shear storage modulus
G_l	Shear loss modulus
MPa	Mega-Pascal
NL	Near Linear
ppm	Parts per million
SL	Step Like
SPEC	Simplified Potential Energy Clock Model
SPECTACULAR	Research version of the SPEC Model
TA	TA Instruments
$\tan(\delta)$	Tangent loss modulus (G_l/G_s)
WLF	Williams-Landel-Ferry

1. INTRODUCTION

Glass-ceramic to metal seals (GcTMS) have become a popular option for hermetic seal designers due to the ability of the glass-ceramic seal to maintain hermeticity over a greater range of pressures and temperatures. Though there are multiple glass-ceramic formulations, belt-processed S-glass (BPS) has been developed to have a coefficient of thermal expansion (CTE) that matches commonly used metals for hermetic seal applications [1]. In this study, one particular lithium silicate glass-ceramic, $\text{Li}_2\text{O}\text{-}\text{SiO}_2\text{-}\text{Al}_2\text{O}_3\text{-}\text{K}_2\text{O}\text{-}\text{B}_2\text{O}_3\text{-}\text{P}_2\text{O}_5\text{-}\text{ZnO}$, is analyzed [1, 2]. Specifically, this paper will consider Step-Like (SL) glass-ceramic with a CTE of 16.8 ppm/ $^{\circ}\text{C}$ (hereafter referred to as SL 16.8). The SL glass-ceramic is so named due to the step-like change in the thermal strain near 250 $^{\circ}\text{C}$ that occurs while heating or cooling the material.

High-fidelity finite-element material models are necessary to allow model-based design and to provide greater understanding of glass-ceramic hermetic seal behavior over a wide temperature range. Currently, the model most suitable to analyzing the viscoelastic behavior of glass-ceramic is the Simplified Potential Energy Clock (SPEC) material model [3-5]. This model was developed for amorphous polymers and has been validated for use with multiple materials including inorganic glass [6]. Since SPEC is currently Sandia's most versatile viscoelastic material model, it was desired to determine if the SPEC model is capable of simulating the viscoelastic behavior of glass-ceramics.

To determine if SPEC is able to capture the behavior of glass-ceramic material, the material model must first be calibrated and then model predictions are compared to validation data sets. Frequency sweeping oscillatory isothermal shear tests were performed to measure the shear storage and loss moduli. The shear and tensile storage and loss moduli were also measured as a function of temperature using a constant frequency oscillatory temperature sweep. Thermal strain was measured at various heating and cooling rates. Lastly, data was obtained from three-point bend creep experiments performed at 460 $^{\circ}\text{C}$ and 550 $^{\circ}\text{C}$ to be used for model validation.

This paper will provide an overview of the experiments performed and brief analysis of the obtained data. Model calibration results will then be presented. Lastly, model predictions will be compared to the available three-point bend creep data. Discussion on model calibration, validation, and areas for further study will be presented.

2. EXPERIMENTAL DATA

Calibrating the SPEC model requires that multiple measurements be made over a broad range of temperatures [6]. Dynamic isothermal torsion tests are performed to measure the shear storage and loss moduli as a function of frequency. These data are useful for constructing a shear master curve. In addition, the temperature dependence of the shear storage and loss moduli were also measured. Tensile storage and loss moduli as a function of temperature are measured using oscillatory three-point bend tests. Thermal strain measurements were made for various cooling and heating rates. This entire data set was used to calibrate the SPEC material model. High temperature three-point bending creep experiments were then performed to provide model validation data.

2.1. Dynamic Torsion Tests

The in-phase and out-of-phase shear moduli were measured in an infinitesimally small strain torsion test using the Anton Paar Modular Compact Rheometer 502 rheometer with a CTD1000 environmental chamber. Inconel torsion fixtures were used in place of stainless steel to avoid warping of the fixtures at temperatures greater than 600 °C and to minimize the CTE mismatch that occurs between the specimen and the fixture. The specimens were nominally 41 mm long with a rectangular cross section of 10 mm by 0.9 mm.

To construct the shear master curve, dynamic torsion tests were performed. The sample was heated from room temperature to 500 °C at 3 °C/min and held for approximately 5 minutes at that temperature to thermally equilibrate prior to starting the frequency sweep. Then the shear storage and loss moduli, G_s and G_l respectively, were measured at frequencies ranging from 0.01 to 10 Hz. Following this, the sample temperature was increased by 50 °C, held constant for approximately 5 minutes, and the frequency scan repeated. By continuing this process, data were collected over a temperature range from 500 to 800 °C. This temperature range was used as the transition temperature was expected to occur around 600 °C. This resulted in a storage modulus (Figure 1) and loss modulus (Figure 2) vs frequency curve for each test temperature. The corresponding loss tangent, $\tan(\delta) = G_l / G_s$, as a function of frequency are calculated for each temperature (Figure 3).

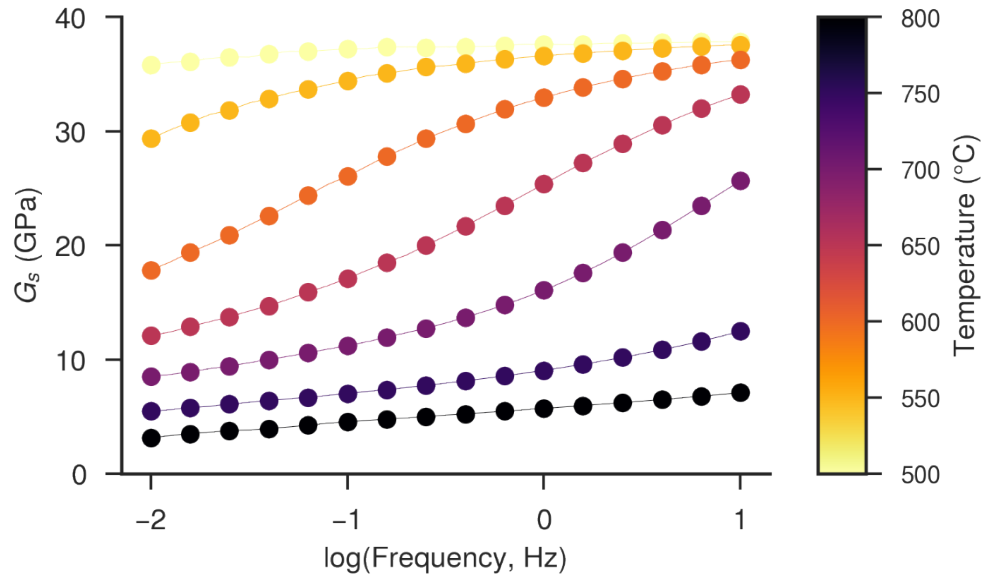


Figure 1. Measured Shear Storage Modulus at Various Temperatures.

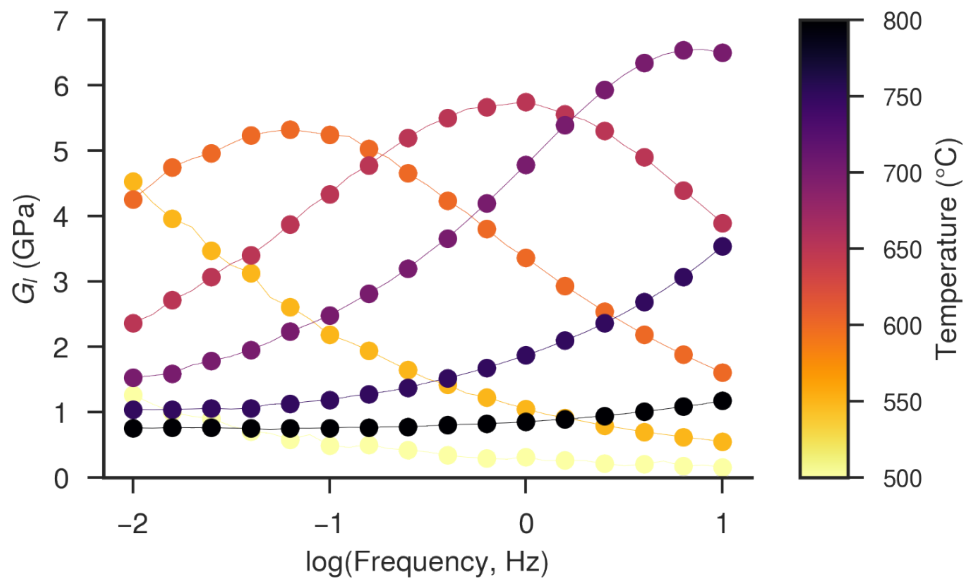


Figure 2. Measured Shear Loss Modulus at Various Temperatures.

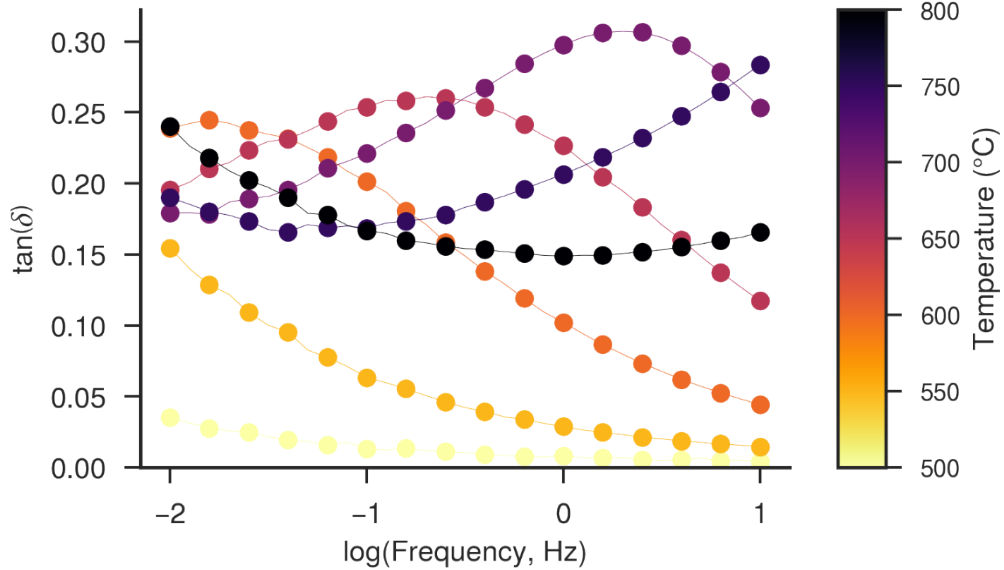


Figure 3. Measured Shear Tan Delta at Various Temperatures.

The storage and loss shear moduli as a function of temperature were measured in an infinitesimally small strain torsion test using the same system that was used for the master curve measurements. This was accomplished by measuring the response by imposing an oscillatory deformation of 0.0005% strain at 1 Hz as the temperature was ramped at 3 °C/min from room temperature to 800 °C. This strain level was confirmed to lie within the linear viscoelastic plateau. The measured temperature dependence of the shear storage and loss moduli are shown in Figure 4 and the measured tan delta is shown in Figure 5. The data shown in these figures were used for model validation.

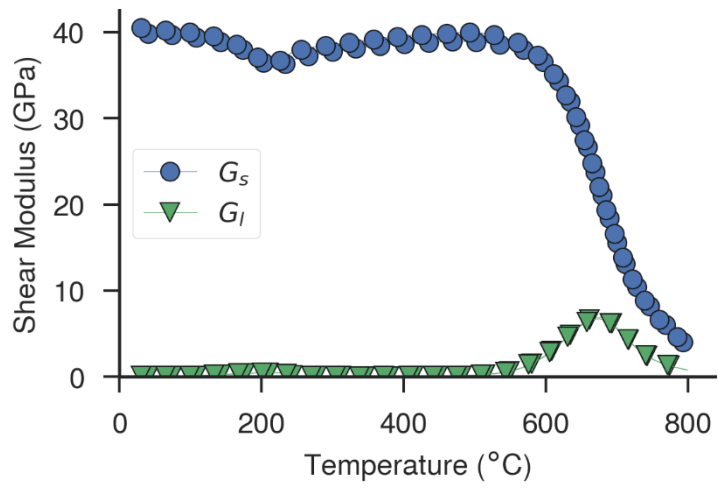


Figure 4. Measured Temperature Dependence of the Shear Storage and Loss Moduli.

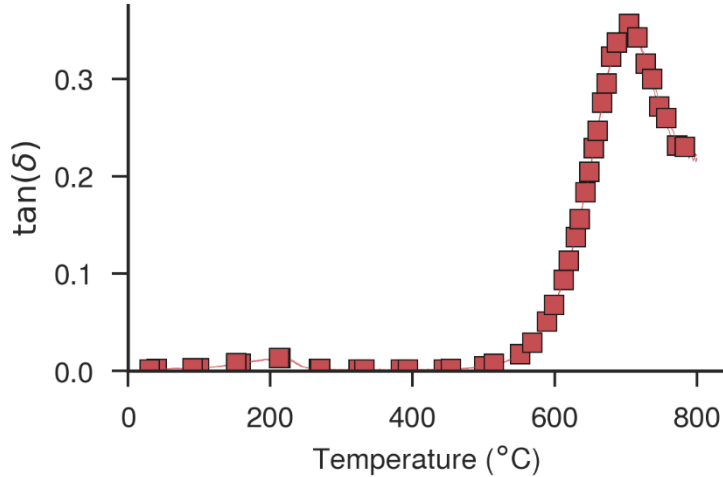


Figure 5. Measured Temperature Dependence of the Shear Tan Delta.

2.2. Dynamic Flexural Tests

The SPEC material model requires calibrating both the shear and bulk relaxation spectrums. Dynamic flexural tests are used for measuring the tensile response and the bulk response can be calibrated using the tensile data and already calibrated shear response. This approach is possible for glass ceramics because these materials are sufficiently compressible to determine with reasonable fidelity the bulk modulus from the shear and Young's moduli. The tensile moduli were measured in a 3-point bending test using the TA Q800 Dynamic Mechanical Analyzer (DMA). This was accomplished by measuring the in-phase and out-of-phase responses while imposing an oscillatory strain of 0.005% at 1 Hz as the temperature was ramped at 2 °C/min from room temperature to 600 °C. The specimens were nominally 55 mm long with a rectangular cross section of 10 mm by 1.1 mm. The temperature dependence was measured twice. The measured tensile storage and loss moduli are shown in Figure 6 and the measured tan delta are plotted in Figure 7.

As observed in the torsional dynamic tests, the glass-ceramics maintain the ability to carry a shear load up to 800 °C. Though it was desired to measure the tensile moduli up to 800 °C, the maximum operating temperature of the TA Q800 is 600 °C. Furthermore, due to limitations of the thermal chamber, the specimens were not annealed prior to testing. The effect of annealing vs not annealing is currently unknown. Also, it is worth noting that the data are very consistent between tests. There is very little difference between each temperature sweep.

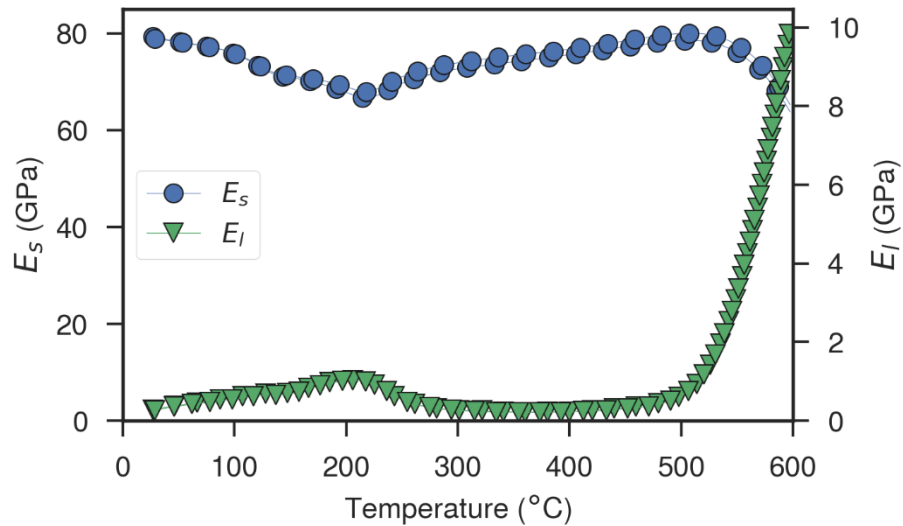


Figure 6. Measured Temperature Dependence of the Tensile Storage and Loss Moduli.

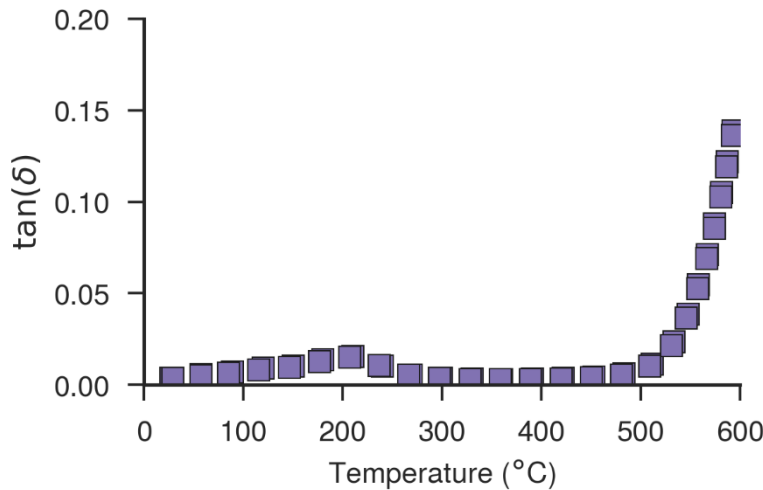


Figure 7. Measured Temperature Dependence of the Tensile Tan Delta.

2.3. Thermal Strain Tests

To provide characterization for the structural relaxation behavior, experiments were conducted to measure the thermal strain changes generated by prescribed temperature histories. The thermal strain data were collected using a Netzsch Expedis Select optical dilatometer using samples nominally 25 mm long with a 5 mm by 5 mm cross-section. Thermal strain for SL glass-ceramic with a nominal CTE of 15.8 ppm/°C was measured. The sample was heated to 750 °C and then cooled at 1, 2, 5, and 10 °C/min to -50 °C. Between each cooling the sample was reheated at 20 °C/min. It is possible that thermal lag occurs in the glass-ceramic sample at this cooling rate but will be considered negligible for the current study. The thermal strain data is shown in Figure 8. Note, the modulus data shown in this report was measured using SL glass-ceramic

with a nominal CTE of 16.8 ppm/ $^{\circ}\text{C}$. This thermal strain data will be used for model calibration due to lack of available data for SL 16.8. During the model calibration, it was assumed that the moduli are not affected by using SL 15.8 glass-ceramic data.

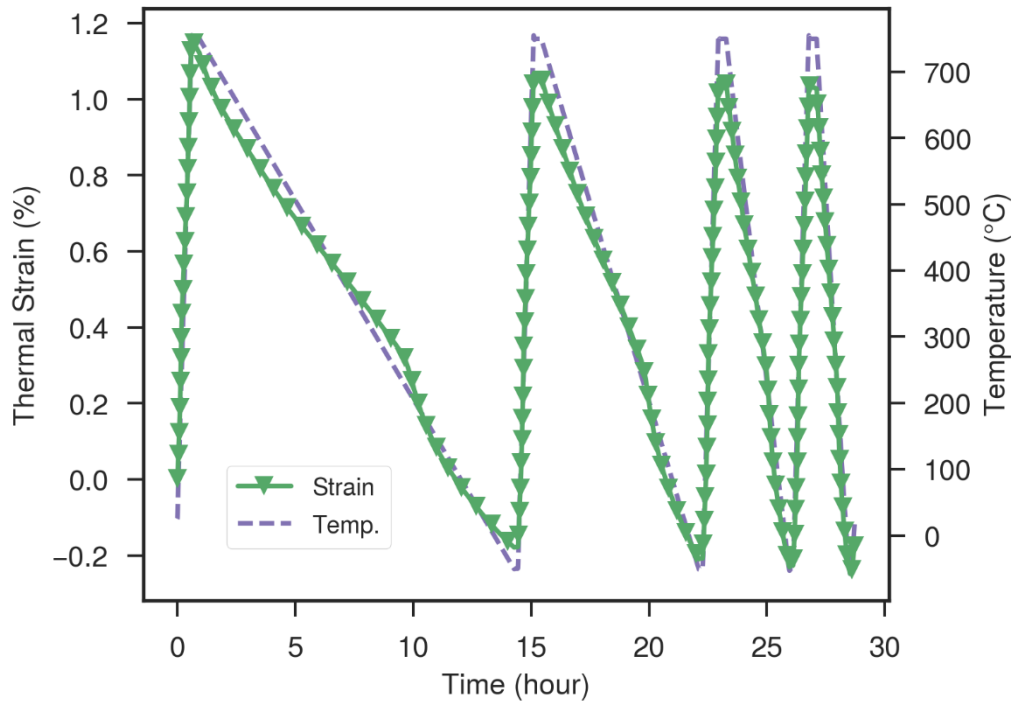


Figure 8. Measured Thermal Strain Data for Various Cooling Rates.

2.4. High Temperature Flexural Creep Tests

Lastly, 3-point bend creep tests were performed to provide a set of data to use for validation of the SPEC material model fit. All tests were performed on the nominally sized 55 mm \times 10 mm \times 1.1 mm glass-ceramic beams using the TA Q800 Dynamic Mechanical Analyzer. Creep was measured for SL 16.8 glass-ceramic. Creep measurements were made at 460 and 550 $^{\circ}\text{C}$. At each temperature, the 3-point bending beam geometries were tested in creep under several different magnitudes of loading ranging from 10 MPa to 90 MPa. Samples were heated from room temperature to the test temperature, held for 10 min and then the load was ramped to the specified test load in 5 seconds and then held constant for 120 minutes. During this time the mid-span creep deflection in the beam was measured as a function of time. The creep data at 460 $^{\circ}\text{C}$ is shown in Figure 9 and the data at 550 $^{\circ}\text{C}$ is shown in Figure 10. The creep compliance data at 460 $^{\circ}\text{C}$ are shown in Figure 11 and at 550 $^{\circ}\text{C}$ are shown in Figure 12.

As can be seen in Figure 10, the 90 MPa test was conducted twice at 460 $^{\circ}\text{C}$. The results for both of these tests are the same within 3%. The same stress magnitudes (10, 30, 50, 70, and 90 MPa) were considered for the 550 $^{\circ}\text{C}$ test but the 90 MPa test specimen broke during loading.

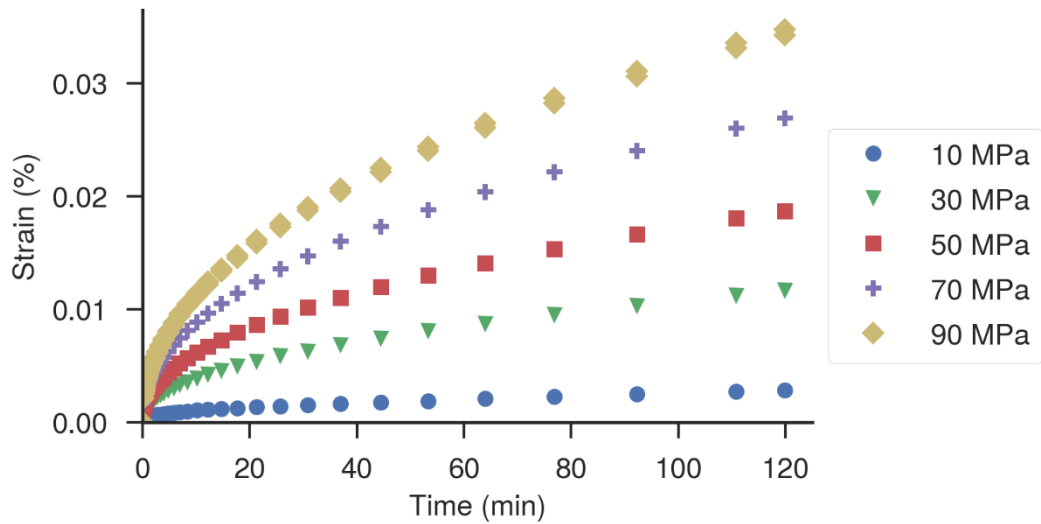


Figure 9. Measured 3-Point Bend Creep at 460 °C at Several Stress Levels

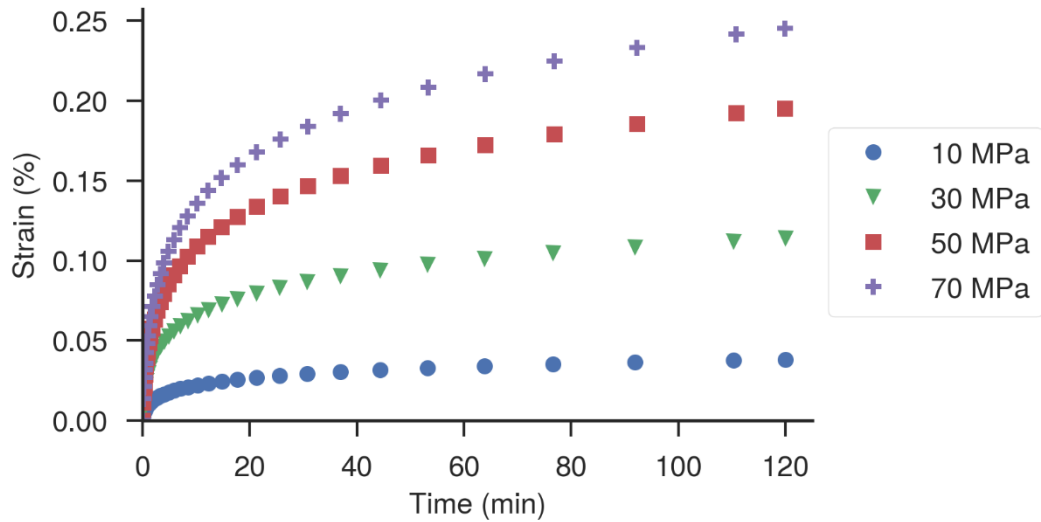


Figure 10. Measured 3-Point Bend Creep at 550 °C at Several Stress Levels

As expected, the creep compliance of the glass-ceramic at 460 °C is lower than the compliance at 550 °C. The creep compliance for the 10 MPa at 460 °C and the 70 MPa at 550 °C samples are anomalously different from the other specimens. Repeat measurements are needed to determine if the behavior at these loads and temperatures are physical or caused by experimental error.

At both temperatures, the creep compliance is nominally the same for each stress level. Though this behavior is indicative of a linear viscoelastic material, further

experiments are needed to determine if deformation induced mobility or other physical phenomena are the reason for the observed anomalous behavior.

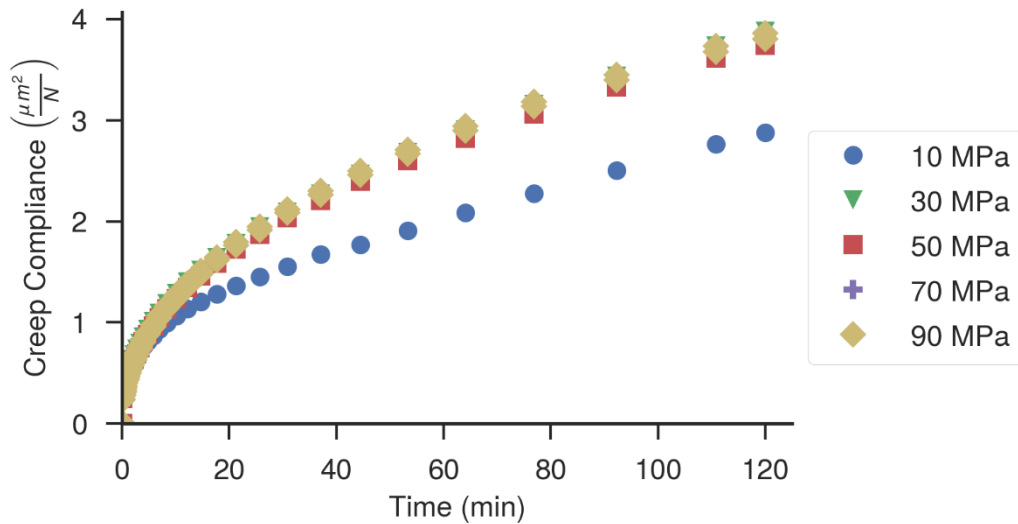


Figure 11. Measured Creep Compliance at 460 °C at Several Stress Levels.

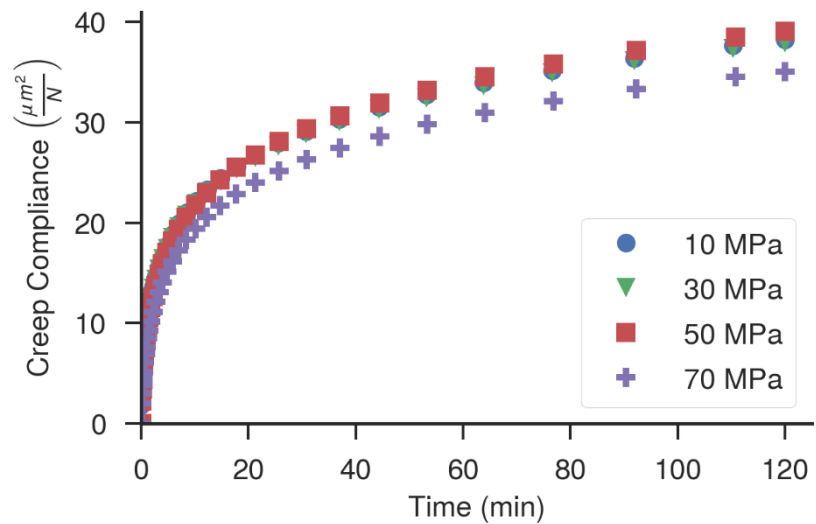


Figure 12. Measured Creep Compliance at 550 °C at Several Stress Levels.

3. MODEL CALIBRATION

The data outlined above in Section 2 was used to calibrate the SPEC material model for SL 16.8 glass-ceramic. A shear master curve was constructed by shifting the shear isothermal frequency sweeps. Glassy and equilibrium shear moduli, as well as the shear Prony series, were calibrated to the shear master curve. The glass and equilibrium bulk moduli and the bulk stretched exponential terms were then calibrated using the 3-point bend temperature sweep. Lastly, the model thermal strain was defined directly using the thermal strain measurements, no SPEC calibration was required.

3.1. Shear Master Curve

A key assumption of the SPEC material model is that the material is thermorheologically simple. This assumption implies that the material behavior exhibits time-temperature equivalence. The time-temperature equivalence can be demonstrated by building a smooth master curve. A shear master curve was created by shifting the frequency of the isothermal shear data obtained in Section 2.1. The data was shifted relative to a reference temperature of 650 °C. This reference temperature was selected based off of the temperature of the peak tan delta response shown in Figure 5. The shear storage and loss moduli master curves are shown in Figure 13 and tan delta is shown in Figure 14.

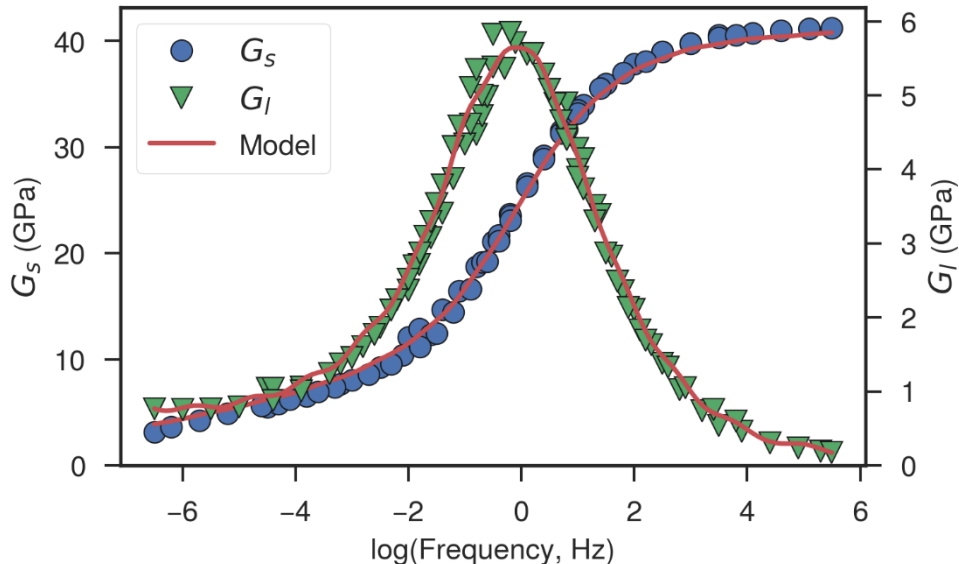


Figure 13. Shifted Shear Storage and Loss Master Curves for a Reference Temperature of 650 °C.

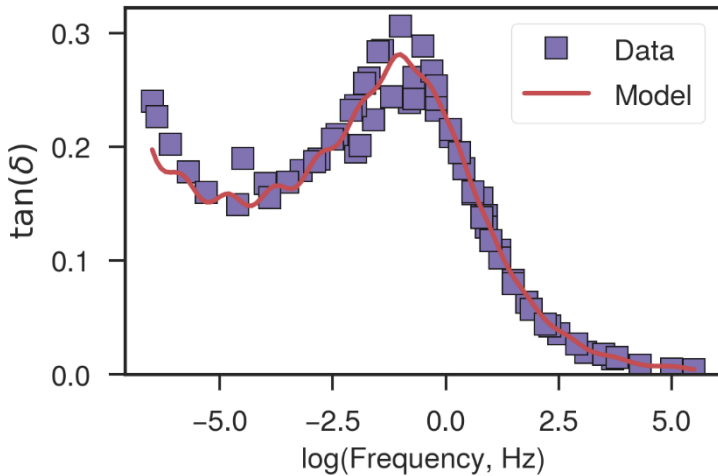


Figure 14. Shifted Master Curve of the Shear Tan Delta for a Reference Temperature of 650 °C.

The shift factors defining these master curves are plotted in Figure 15. The Williams-Landel-Ferry (WLF) form was fit to the data and is also shown in the image. The value of the two coefficients are $C_1 = 16$ and $C_2 = 2,000$ °C. It can be seen in the image that the WLF form fits the shifted values well across the temperature range of the data although the large value of C_2 suggests that a different functional form may be preferable.

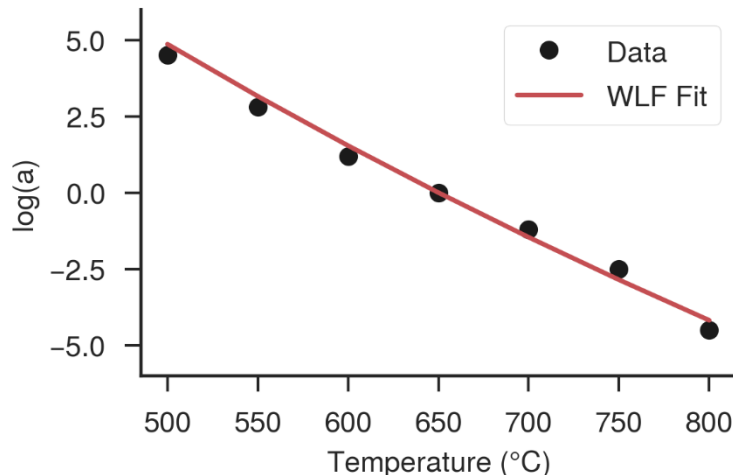


Figure 15. Log(a) Shift Factors for a Reference Temperature of 650 °C and the Williams-Landel-Ferry Fit.

The vertical shifts used in constructing the shear master curve are shown in Figure 16. The predicted shift factors represent the ratio of the reference temperature to the temperature where the data were collected. For temperatures less than 650 °C, small vertical shifts were necessary to construct a smooth master curve, particularly for the storage master curve. For temperatures greater than 650 °C, only the curve for 700 °C required a vertical shift. The 700 °C shift was required to construct a smooth loss

master curve. Though vertically shifting the data to construct a master curve may indicate that the material is thermorheologically complex [7], it has been shown that small vertical shifts have little effect on the thermorheological simplicity assumption [8-10].

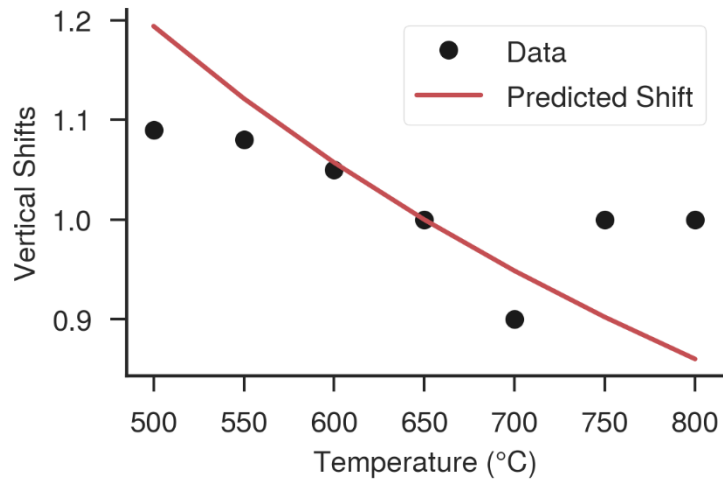


Figure 16. Vertical Shift Factors Used when Constructing the Shear Master Curve.

3.2. 3-Point Bend Temperature Sweep

After the shear spectrum was calibrated, the 3-point bend temperature sweep data shown in Section 2.2 was used to calibrate the bulk spectrum. Since data was only taken from room temperature to 600 °C, the model can only be calibrated over that temperature range. Thus the accuracy of the bulk response above 600 °C is unknown. A comparison of the storage and loss moduli are shown in Figure 17 and a comparison of the tan delta is shown in Figure 18.

A one element uniaxial tension model was used for calibration. The model was cooled from 1,000 °C to room temperature at 2 °C/min and then reheated to 600 °C at 2 °C/min. For calibration purposes, it was assumed the bulk response followed a stretched exponential form. The bulk τ and β was adjusted to capture the shape of the relaxation spectrum. The glassy bulk modulus and the slope of the glassy bulk modulus were adjusted to approximate the room temperature modulus.

When using a stretched exponential form for the bulk spectrum and a Prony series for the shear spectrum, SPEC will calculate a Prony series for the bulk spectrum based on the relaxation times defined for the shear spectrum. This fitting resulted in negative Prony terms. The negative Prony terms were iteratively removed and the Prony series adjusted to produce a similar spectrum and maintain that the Prony series summed to one. The final bulk spectrum used a Prony series with relaxation times as defined from the shear spectrum.

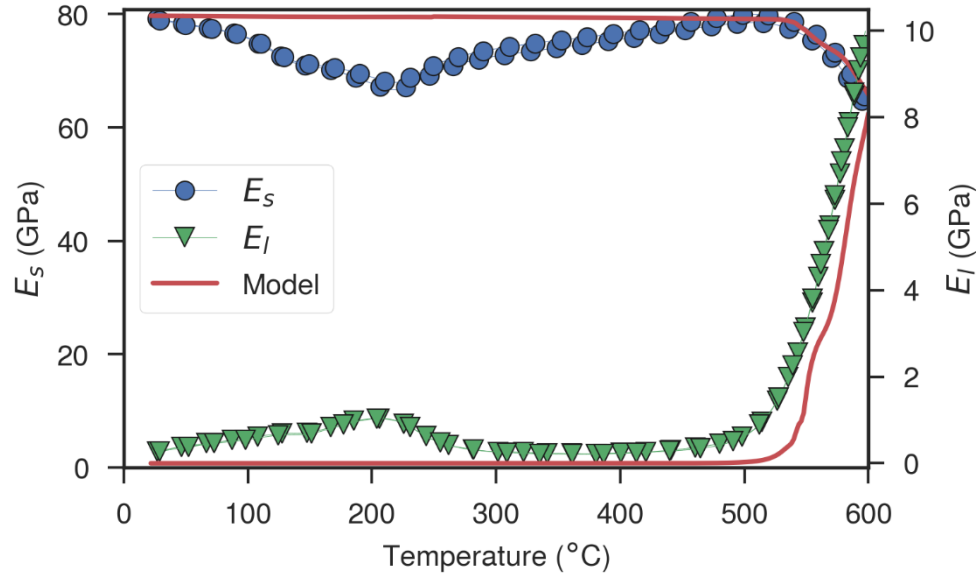


Figure 17. Comparison Between Measured Storage and Loss Moduli and the SPEC Model Fit for the 3-Point Bend Temperature Sweep.

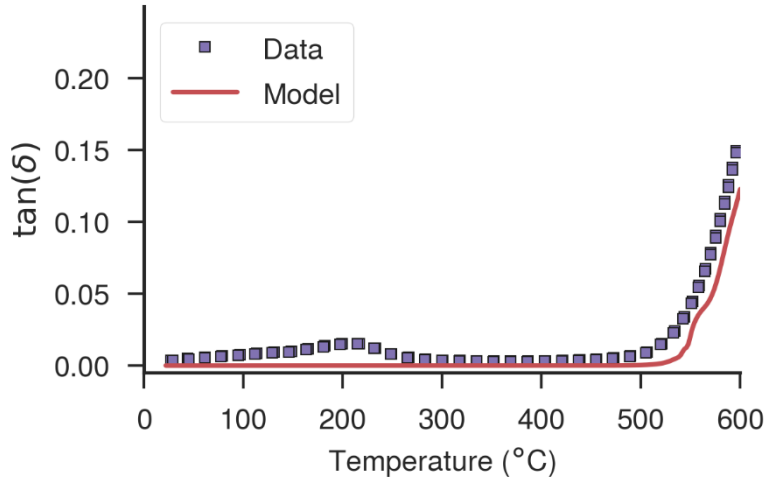


Figure 18. Comparison Between Measured Tan Delta and the SPEC Model Fit for the 3-Point Bend Temperature Sweep.

3.3. Thermal Strain

For other glasses and polymers, thermal strain from different heating and cooling rates can be useful for calibrating the shape of the volumetric spectrum [5-6]. The thermal strain data outlined in Section 2.3 does not exhibit traditional glass transition behavior near the reference temperature. The thermal strain response is linear until approximately 250 °C when the α - β inversion between low- and high-Cristobalite occurs [1]. The current implementation of SPEC makes capturing the step-like

behavior at the α - β inversion impossible. Therefore, to capture the correct thermal strain response, the volumetric CTE parameters in SPEC are set to zero and a thermal strain function is explicitly defined. The shortfall with this approach is that thermal strain is an explicit function of temperature, and it will not depend on cooling/heating rates through the glass transition.

A comparison of the model prediction with data is shown in Figure 19. The data shown is for the increment where the sample was cooled at 5 °C/min from 750 °C to -55 °C, held at -55 °C for 10 minutes, and reheated at 20 °C/min to 750 °C. The cooling and heating data are shown in blue and red. The model exhibits the correct thermal strain response during cooling but does not capture the hysteresis in the data near the α - β inversion. This implies that the volumetric spectrum may need further refining in this temperature range.

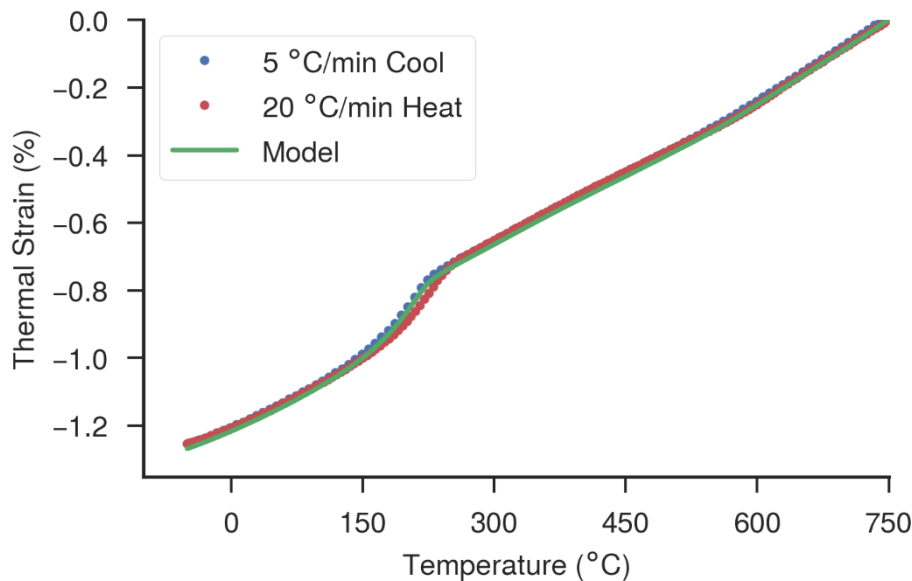


Figure 19. Comparison of the Experimentally Measured Thermal Strain and the Model Predicted Thermal Strain.

3.4. SPEC Model Calibration

After collecting the characterization data and calibrating the SPEC model as described in Sections 3.1 – 3.3, a single set of material properties was identified. The non-zero SPEC model inputs are defined in Table 1. The Prony relaxation times and the normalized Prony weights for both the bulk and shear spectrums are listed in Appendix A. These material parameters are used for the model results shown in the next section.

Table 1. SPEC Model Parameters for SL 16.8 Glass-Ceramic.

Physical Description	Parameter	Value
Glassy bulk modulus	K_g (GPa)	25.8
Slope of the glassy bulk modulus (in temperature)	dK_g/dT (GPa/°C)	0.001
Equilibrium bulk modulus	K_r (GPa)	6.0
Slope of the equilibrium bulk modulus (in temperature)	dK_r/dT (GPa/°C)	-0.0059
Glassy shear modulus	G_g (GPa)	40.0
Slope of the glassy shear modulus (in temperature)	dG_g/dT (GPa/°C)	-0.003
Equilibrium shear modulus	G_r (GPa)	0.025
Reference temperature	T_{ref} (°C)	650
Stress-free temperature	T_0 (°C)	1,000
WLF C_1	C_1	60
WLF C_2	C_2 (°C)	2,000

4. MODEL VALIDATION

In the previous section, the calibration for SL 16.8 glass-ceramic was presented. In order to assess the validity of the model prediction comparisons were made to two sets of available experimental data. First, oscillatory shear temperature sweeps were used to test the accuracy of the calibrated shear spectrum. Second, high temperature 3-point bend creep data was used to assess the overall behavior of the material calibration. In this section, comparisons between model and experiment are shown and the results are discussed.

4.1. Shear Temperature Sweep

An one element oscillatory simple shear model was used to predict the temperature dependence of the shear moduli. The model was cooled at 3 °C/min from the stress free temperature (1,000 °C) to room temperature. During the cooldown, an infinitesimally small oscillatory shear is applied with a frequency of 1 Hz. The storage and loss moduli are then calculated from the stress-strain response of the model.

Comparisons for the storage and loss moduli are shown in Figure 20 and comparisons of tan delta are shown in Figure 21.

The model prediction for the storage modulus is quite good over the temperature range of the data. An equilibrium shear modulus is required in the SPEC model, which here may represent the solid skeleton behavior of the percolated network of crystalline phase(s). Since data is unavailable at higher temperatures to experimentally determine the equilibrium shear modulus, the model prediction at 800 °C is based on a *guess* of what the actually equilibrium shear modulus is. The model fits the data well through the transition region. From approximately 500 °C to room temperature, the model prediction does not follow the trend of the data. As the temperature decreases and the Cristobalite goes through the α - β inversion, the storage modulus reaches a minimum and then climbs again. The model prediction does not capture this decrease and assumes the material continues to increase in stiffness as the temperature decreases.

The model predicts the shape of the loss modulus well during transition. The temperature range of the transition is captured well though the peak magnitude of the loss modulus is lower by approximately 1 GPa. Similar to the storage modulus, the model does not capture the behavior of the material during the α - β inversion of the Cristobalite.

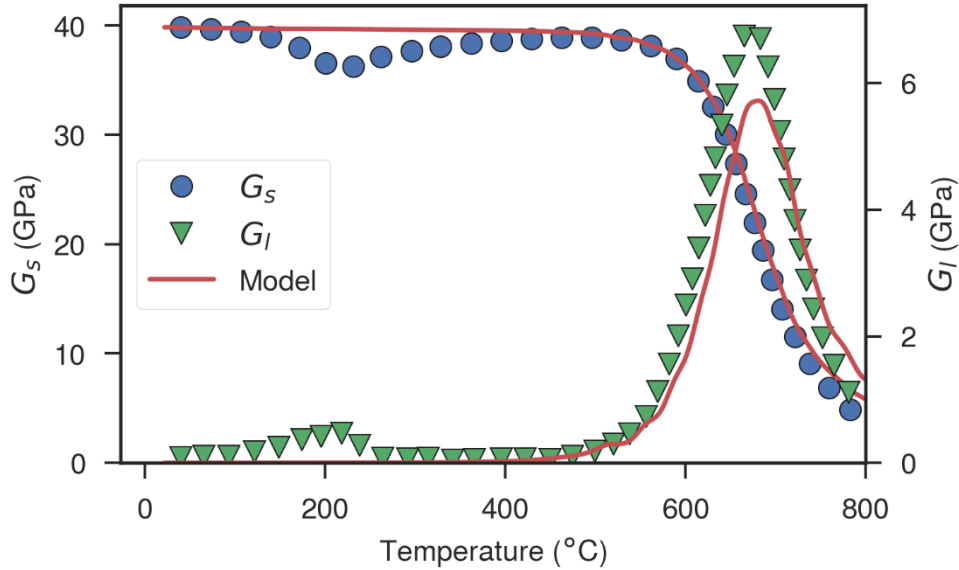


Figure 20. Comparison Between the Measured Shear Storage And Loss Moduli and the SPEC Model Predictions for the Shear Temperature Sweep.

The model predictions of tan delta are good as well. From the loss modulus predictions, there exists a small shift in temperature during the transition and the peak of tan delta is under estimated. The model prediction above 750 °C exhibits some noisy behavior. Additional data at temperatures about 800 °C would allow further refinement of the Prony series that is used for the shear spectrum.

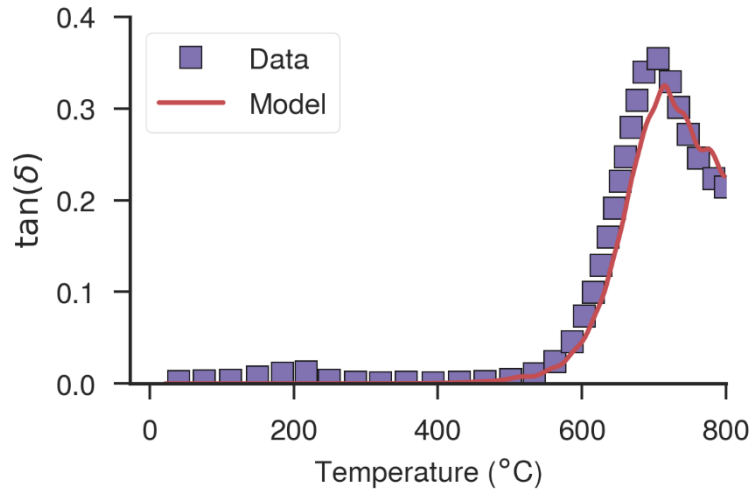


Figure 21. Comparison Between the Measured Tan Delta and the SPEC Model Predictions for the Shear Temperature Sweep.

4.2. High Temperature Creep

Predictions from the calibrated SPEC model were compared to the high temperature creep data shown in Section 2.4. A schematic of the 3-point bend model geometry is shown in Figure 22. The average of the measured dimensions for all samples tested were used for the model dimensions. The dimensions of the model are 55 mm x 10.11 mm x 1.08 mm. The span of the bottom supports is 50 mm. Symmetry (quarter) was applied at the center of the span and through the width of the model. The average element size was 0.25 mm with six elements through the thickness of the beam. The model consisted of 20,880 uniform-gradient hexahedral elements and 25,463 nodes. The supports are stainless steel and are assumed to remain elastic. Contact was modeled between the glass-ceramic and stainless steel with an interfacial friction coefficient assumed to be 0.3.

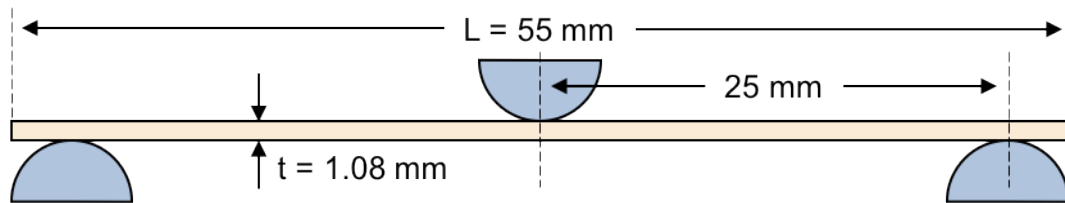


Figure 22. Schematic of the 3-Point Bend Model.

The 3-point bend model was cooled at 2 °C/min from 1,000 °C to room temperature and reheated at 2 °C/min to the creep temperature (460 or 550 °C). The temperature was then held constant at the creep temperature for 10 minutes and the load was then applied in 5 seconds. The load was held constant for 120 minutes. The load was applied through a distributed force on the top surface of the top roller.

Model predictions for 3-point bend creep at 460 °C are compared to experimental data in Figure 23 and Figure 24. The model results for 70 MPa are omitted due to unexplainable model behavior. While the model predicts the measured strain at 120 minutes, the shape of the strain profiles are different. The shapes of the curves differ more as the load increases.

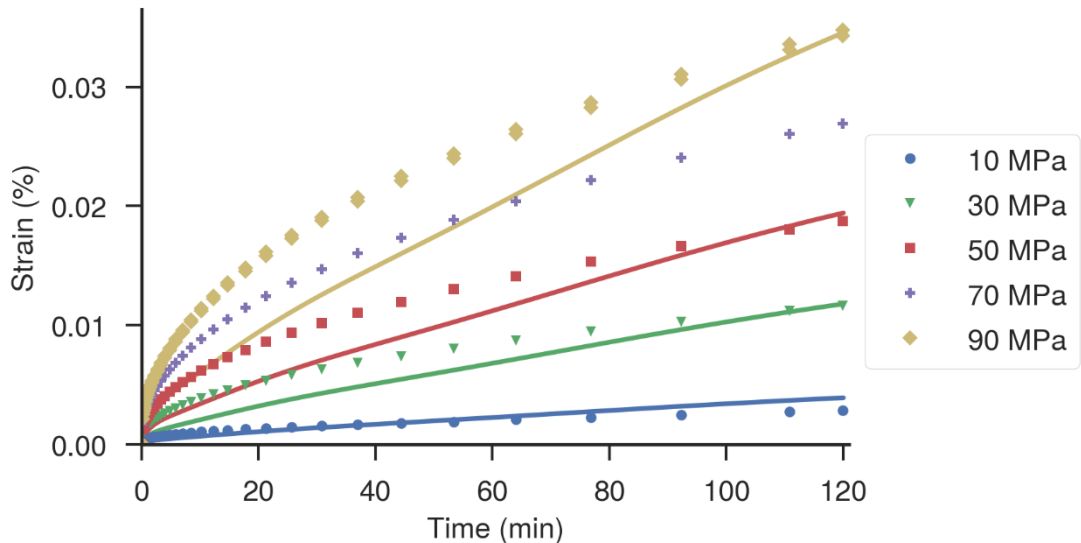


Figure 23. Comparisons Between Measured Creep Strain (symbols) and SPEC Model (solid lines) Predictions for 3-Point Bend Creep at 460 °C.

The model generally underpredicts the compliance. At approximately 60 minutes there is a small change in the slope of the compliance. At the 120 minute mark, the model is predicting nearly the same compliance. It is predicted that past 120 minutes, the model would begin to overpredict the creep compliance. Though the model predictions match the data near 120 minutes, this does not imply the model is accurately capturing the physics of the experiment. That the model predictions intersect the experimental data at 120 minutes is likely serendipitous. The finite tensile loss modulus at 460 °C (Figure 17) is likely a dominant factor in the model overpredicting the relaxation.

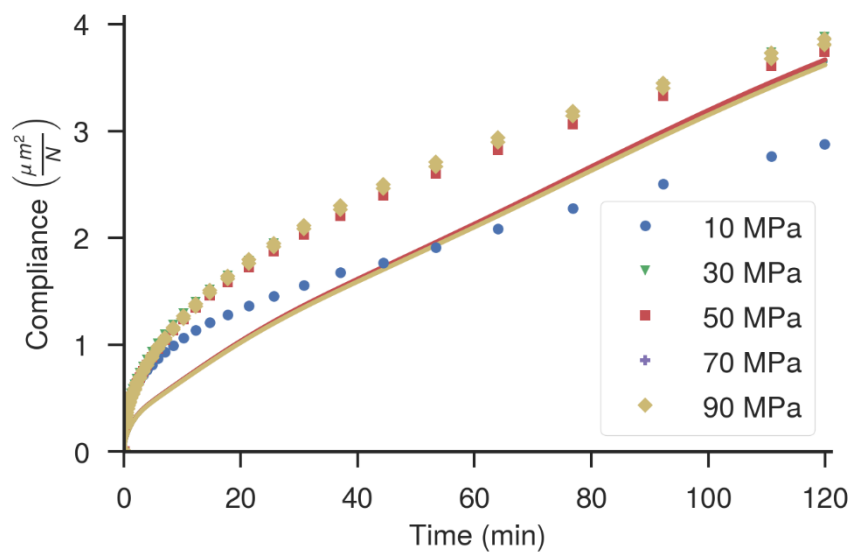


Figure 24. Comparisons Between Measured Creep Compliance (symbols) and the SPEC Model (solid lines) Predictions for 3-Point Bend Creep at 460 °C.

Model predictions for 3-point bend creep at 550 °C are compared to experimental data in Figure 25 and Figure 26. At 550 °C the glass-ceramic SPEC model underpredicts the creep. At 120 minutes, the model is approximately 50% less compliant for both the strain and compliance predictions. Though the predicted magnitude is wrong the shape of the model predictions is similar to that of the data.

The model underpredicting the creep behavior at 550 °C may be due to a combination of factors. First, as can be seen in Figure 20, the model underpredicts the loss moduli at 550 °C in the shear temperature sweep. Because of this, the model will not have the same amount of relaxation as observed in the experiment. Second, the volumetric Prony weights for relaxation times greater than 0.2 seconds are less than 1.0e-3. This suggests that at these relaxation times there is little contribution from the volumetric spectrum. The combination of these two factors are likely the source of the model underpredicting the compliance in the glass-ceramic.

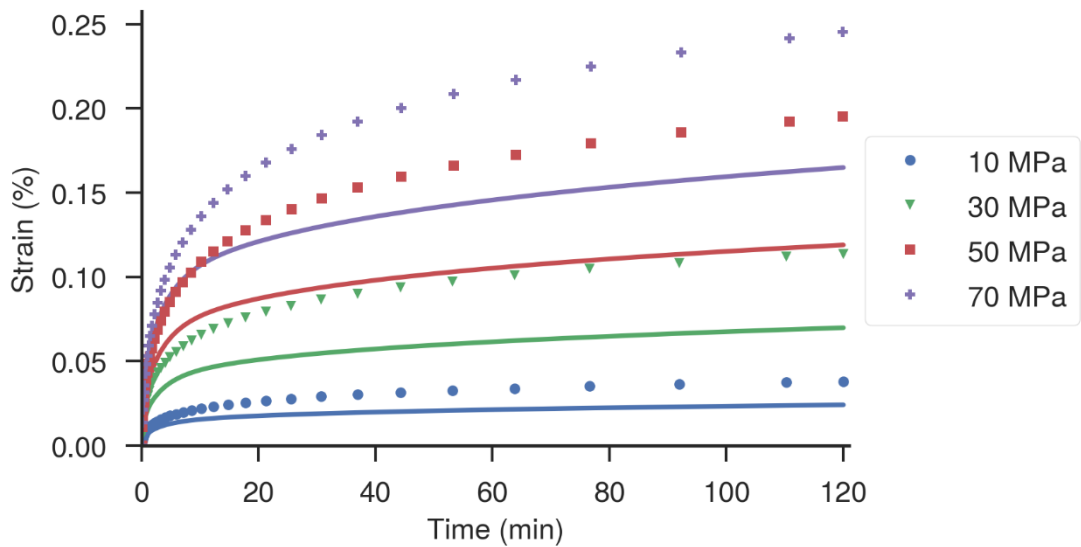


Figure 25. Comparisons Between the Measured Creep Strain (symbols) and the SPEC Model (solid lines) Predictions for 3-Point Bend Creep at 550 °C.

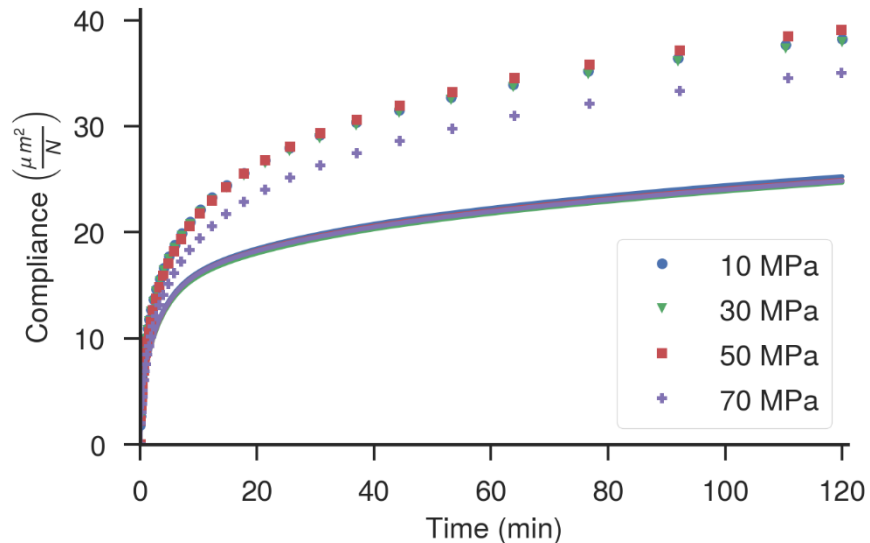


Figure 26. Comparisons Between the Measured Creep Compliance (symbols) and the SPEC Model (solid lines) Predictions for 3-Point Bend Creep at 550 °C.

4.3. Validation Summary

The SPEC material model was fit to glass-ceramic data and was then used to predict the oscillatory shear temperature sweep and the 3-point bend creep data within a reasonable degree of error. Given that glass-ceramic is a composite material with multiple phases and that it is likely thermorheologically complex, the model does behave better than originally expected. Re-calibration to a data set across a broader temperature range would likely help reduce the error in the model predictions. Though these results suggest that SPEC may potentially be used to predict the stress in a GcTMS, only additional experimental results will be to prove if SPEC is applicable. Suggestions for future work are presented in the following section.

5. FUTURE WORK

This work has shown that SPEC *may* be capable of making predictions of glass-ceramic behavior with engineering accuracy. To determine if this is truly the case further effort is required. New experimental data and further model calibration and validation are all required. Following are suggestions for future experimental and modeling efforts.

5.1. Experimental

Validation of the applicability of SPEC to modeling glass-ceramics is dependent on data from various experiments. Though experimental challenges still exist, particularly related to the high temperature behavior of glass-ceramics, various experiments can still be performed to gather useful data. Suggestions for future experimental work include:

1. Measure shear master curve data to approximately 950 °C or until equilibrium like response is obtained. The machine used to obtain the data shown in Section 2.1 is capable of temperatures up to 1,000 °C. Additionally, measure the material response at smaller temperature increment (smaller increments than 50 °C).
2. Increase the maximum temperature of the oscillatory shear temperature sweep to at least 900 °C.
3. Measure 3-point bend creep at 400 °C, 500 °C, and 600 °C for various lengths of time (i.e. 2 hours and 4 hours). Also, selectively repeat tests to reduce uncertainty in the experimental measurements.
4. If possible, assess the effect of annealing vs. not annealing samples prior to oscillatory shear temperature sweeps, 3-point bend temperature sweeps, as well as other experiments.
5. If possible, make material samples that are only the amorphous glass phase of the glass-ceramic. Measure the shear and flexural properties as well as the thermal strain behavior of this material.
6. Measure properties (shear, flexural, thermal strain) for NL glass-ceramic. Compare viscoelastic data between NL and SL glass-ceramics.
7. Make simple GcTMS with no electrical contacts. With these simple GcTMS, do the following:
 - a. Infer glass-ceramic residual stress using the indentation fracture method.
 - b. Measure glass-ceramic residual stress using photoluminescence spectroscopy.

5.2. Modeling

Updates to the calibration and the material model are dependent on data showing the need for further development. Given additional data, following are suggestions for future model refinement, areas of investigation, and model development activities.

1. Update the current calibration with data collected at higher temperatures. Assess the effect of calibrating with higher temperature data.
2. Calibrate SPEC to NL glass-ceramic data. Compare NL calibration and behavior to SL glass-ceramic. Also, investigate SPEC applicability to different CTE SL and NL glass-ceramics, i.e. is changing the thermal strain function sufficient to capture material behavior?
3. Calibrate SPECTACULAR to available data. SPECTACULAR is the next version of the SPEC material model that is capable of using different relaxation times for the shear and bulk spectrums. Investigate if the uncoupling of relaxation times between the shear and volumetric spectrums is beneficial.
4. Determine if it is possible to use the filler volume fraction functionality in SPEC to model the α - β inversion of the Cristobalite.
5. Using SPEC or SPECTACULAR, determine if it is possible to separate the different phases of the material, similar to what has been done using a generalized Maxwell model [7].

6. CONCLUSION

Glass-ceramic hermetic connectors are becoming more common in Sandia related applications. More advanced finite-element material models are required to enable model-based design and provide evidence that the hermetic connectors can meet design requirements for long-term applications. Available glass-ceramic data was used to calibrate the Simplified Potential Energy Clock model. A shear master curve was constructed to identify shear spectrum parameters, the volumetric relaxation spectrum was characterized using oscillatory 3-point bend data, and the thermal strain was defined explicitly with measured data. It was shown that the model could predict oscillatory shear temperature sweep data well from 500 to 800 °C. Below 500 °C, the model is not able to capture behavior related to the α - β inversion of the Cristobalite. The model is able to predict 3-point bend creep data at 460 °C within engineering accuracy but underpredicts the creep data at 550 °C. Suggestions for further data collection and model development were presented. Overall, SPEC was able to an admirable job of predicting glass-ceramic behavior at elevated temperatures. Further calibration may show that SPEC is capable of making predictions with increased quantitative accuracy.

REFERENCES

1. S. Dai, M. A. Rodriguez, J. J. M. Griego. Sealing glass-ceramics with near linear thermal strain, Part I: Process development and phase identification. *J. Am. Ceram. Soc.*, 2016, Pages 3719-3725.
2. M. A. Rodriguez, J. J. M. Griego, S. Dai. Sealing glass-ceramics with near-linear thermal strain, Part II: Sequence of crystallization and phase stability. *J. Am. Ceram. Soc.*, Volume 99, Issue 11, 2016, Pages 3726-3733.
3. J. M. Caruthers, D. B. Adolf, R. S. Chambers, P. Shrikhande. A thermodynamically consistent, nonlinear viscoelastic approach for modeling glassy polymers. *Polymer*, Volume 45, 2004, Pages 4577-4597.
4. D. B. Adolf, R. S. Chambers, J.M. Caruthers. Extensive validation of a thermodynamically consistent, nonlinear viscoelastic model for glassy polymers. *Polymer*, Volume 45, 2994, Pages 4599-4621
5. D. B. Adolf, R. S. Chambers, M. A. Neidigk. A simplified potential energy clock model for glassy polymers. *Polymer*, Volume 50, Issue 17, 2009, Pages 4257-4269.
6. R. S. Chambers, R. Tandon, M. E. Stavig. Characterization and calibration of a viscoelastic simplified potential energy clock model for inorganic glasses. *J. Non-Cryst Solids*, Volume 432, 2016, Pages 545-555.
7. S. P. C. Marques, G. J. Creus. Computational Viscoelasticity. Springer, Berlin, 2012.
8. J. Dealy, D. Plazek. Time-temperature superposition – A Users Guide. *Rheology Bulletin*, July 2009.
9. E.T.J. Klompen, L.E. Govaert. Nonlinear viscoelastic behavior of thermorheologically complex materials. *Mech. Time Depend. Mater.*, Volume 3, 1999, Pages 49-69.
10. R. L. Bagley. The thermorheologically complex material. *Int. J. Engng. Sci.*, Volume 29, Issue 7, 1991, Pages 797-806.

APPENDIX A: PRONY TIMES AND WEIGHTS

The normalized Prony weights for the shear and volumetric spectrums are listed below with their associated relaxation times.

Relaxation Times (s)	Normalized Shear Prony Weights	Normalized Volumetric Prony Weight
1.00E-06	2.35E-03	1.78E-02
1.00E-05	1.17E-02	2.96E-02
1.00E-04	2.83E-03	2.32E-02
2.00E-04	1.86E-02	9.86E-02
2.00E-03	3.90E-02	2.50E-01
1.00E-02	2.14E-02	1.37E-01
2.00E-02	5.64E-02	2.78E-01
1.00E-01	1.07E-01	1.65E-01
2.00E-01	1.06E-02	0
5.01E-01	1.47E-01	0
2.00E+00	1.44E-01	0
5.01E+00	8.73E-03	2.34E-04
1.00E+01	1.34E-01	0
5.01E+01	5.25E-02	0
1.00E+02	3.96E-02	0
5.01E+02	4.39E-02	0
1.00E+03	1.54E-02	0
5.01E+03	3.18E-02	0
1.00E+04	1.02E-02	0
5.01E+04	2.41E-02	0
1.00E+05	9.00E-03	0
5.01E+05	1.95E-02	0
1.00E+06	1.02E-02	0
5.01E+06	1.01E-02	0
1.00E+07	3.05E-02	0
0	0	0
0	0	0
0	0	0
0	0	0
0	0	0

DISTRIBUTION

1	MS0346	Kurtis Ford	01556 (electronic copy)
1	MS0346	Diane Peebles	01556 (electronic copy)
1	MS0346	Brenton Elisberg	01556 (electronic copy)
1	MS0346	Scott Grutzik	01556 (electronic copy)
1	MS0523	Kevin Ewsuk	02631 (electronic copy)
1	MS0781	Mark Retter	06621 (electronic copy)
1	MS0825	Jeff Payne	01513 (electronic copy)
1	MS0840	John Emery	01554 (electronic copy)
1	MS0840	Brian Lester	01554 (electronic copy)
1	MS0840	Kevin Long	01554 (electronic copy)
1	MS0889	Antoun Sumali	01851 (electronic copy)
1	MS0889	Dave Reedy	01556 (electronic copy)
1	MS0958	Michael Kelly	01833 (electronic copy)
1	MS1411	Mathias Celina	01853 (electronic copy)
1	MS9042	Arthur Brown	08259 (electronic copy)
1	MS0899	Technical Library	9536 (electronic copy)



Sandia National Laboratories